Pseudo-elastic characterization of elastomeric materials by cyclic multi-axial loading tests

Giacomo Palmieri[1], Gianluca Chiappini[1], Marco Sasso[1], Dario Amodio[1]

[1]*Department of Mechanics, Università Politecnica delle Marche, Italy*
E-mail: *g.palmieri@univpm.it, g.chiappini@univpm.it, m.sasso@univpm.it, d.amodio@univpm.it*

Keywords: Mullins effect, pseudo-elasticity, elastomeric materials, cyclic tension tests.

SUMMARY. One of the principal inelastic effects of rubber-like materials is a particular damage phenomenon called Mullins effect. This is visible when cyclic tension tests are performed with increasing values of deformation. Material is deformed up to a fixed strain value and then unloaded. When a second load is applied it is possible to observe a stress softening effect. In the present work uniaxial and equibiaxial cyclic tension test data will be presented. In both tests optical methods have been used for strain measurement. Experimental data have been successively introduced in a numerical procedure that permitted to extract the best material parameters for two of the most known pseudo-elastic models, accounting for both stress-softening behaviour and residual strain.

1 INTRODUCTION

The theory of isotropic elasticity of incompressible materials has been widely used to describe the mechanical behaviour of rubber-like materials. Their particular stress-strain response shows very large strains with strongly non-linear behaviour. This theory is the basis of several constitutive models, said hyperelastic, based on the definition of different strain energy functions[1-3]. A comparison between 5 different hyperelastic constitutive models (Mooney-Rivlin, Ogden, Neo Hooke, Yeoh, Arruda-Boyce) was proposed by Sasso et al. [4]. In the same paper it is also given a procedure to extract material dependent parameters from uniaxial and equibiaxial tests data.

Besides hyperelasticity, several elastomers exhibit some inelastic phenomena, e.g. hysteresis, permanent set and the Mullins effect. The last effect consists in a change of material properties between its original state (unstretched) and after the material has been subjected to a load. It was firstly observed and studied by Mullins and Tobin [5,6]. They idealized that rubber could exist in two phases: a “hard phase” and a “soft phase”. When the material is virgin it shows only the hard phase, but, when greater and greater deformation is applied, more and more rubber degrades in the soft phase. A typical cyclic loading path where Mullins effect is evident is represented in figure 1 in terms of stress-strain curves. On the initial loading (OaA) the virgin material exhibits a relatively stiff response. When the material is subsequently unloaded (AdO), then reloaded (OdA), the stress-strain curve follows a significantly softer path until the point of max deformation previous applied (A) is reached for the second time. Continuing to increase further on the stretch, the stress-strain curve will return to follow the primary path (AbB) until next unload is performed (BeO), and so on. With “primary path” is indicated the curve OaAbBc that is the typical hyperelastic path without stress softening and viscous effects.

Several micro-mechanics explanations have been proposed on this effect; anyway the model proposed by Ogden and Roxburgh [7] for Mullins effect and the extension of this model also to the inelastic behaviour of permanent set by Dorfmann and Ogden [8] are phenomenological approaches, where the physical structure of the material is not taken into account. It follows that these theories can be applied to all materials that show Mullins effect with possible permanent set. Since the material response is governed by different forms of strain energy function on primary loading and unloading, these models are referred as pseudo-elastic.

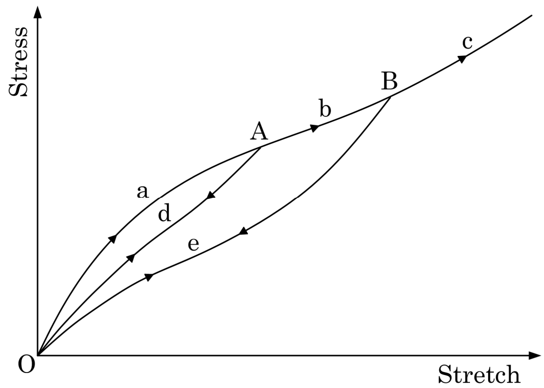

Figure 1: Mullins effect

Most of the works in this topic focalized on uniaxial tension and few information are available for multiaxial tensional states [9-14]. In this paper, an approach where both uniaxial and equibiaxial test data are used in a coupled way to calibrate pseudo-elastic models is proposed. To this purpose a series of tests of cyclic loading at increasing levels of stretch in uniaxial and equibiaxial tension have been carried out. Uniaxial tension tests were performed by means of a standard tensile machine, whereas for equibiaxial tension a rig developed by authors [15] was adopted to perform cyclic bulge tests. In both experimental set-up optical methods were applied to measure the strain field on the specimens. These techniques are not invasive and well suited to be used when large stretches are reached.

Experimental data are then input into a Matlab® procedure where material parameters of the theoretical pseudo-elastic model are iteratively changed in order to minimize the error between test and numerical data. As both uniaxial and equibiaxial data are included in this minimization algorithm, the resulting calibrated model is able to describe the material response in a general tensional state.

2 EXPERIMENTAL TESTS

In order to describe the material behaviour as generally as possible, two different load distributions are considered: uniaxial and equibiaxial extensions. In fact it may happens that a model calibrated from only one load distribution could give inaccurate or instable representations of different tensional states. The method proposed by authors in this paper involves in the inverse procedure of material characterization data of uniaxial and equibiaxial tests in a coupled way. In this section a quick description of the test rigs and experimental methodologies is given, for both uniaxial and equibiaxial extension tests.

Uniaxial stretching tests are performed on dumbbell specimens with a thickness of 1.7 mm. The gauge lenght of the specimen, that is the part whit maximum and uniform deformation, is clearly delimited by two white markers. This zone has a length of 40 mm and a width of 9 mm. The test rig is composed by an electro-mechanical testing machine Zwick Z050 and a high resolution video-extensometer.

Load is measured by a 5kN load cell, the displacement, that is the engineering strain, is measured by the crosshead LVDT, while the true strain in the "useful" part of the specimen is measured by the video extensometer comparing distances between markers along time. Two tests are performed with this rig: the first one is a quasi-static monotonic loading up to a stretch greater than 2 and at a strain rate in the order of 10^{-3} s^{-1}. Data of this test are used to calibrate the hyperelastic model in order to know the primary path of the material in its virgin state. A second test is performed applying cyclic loading and unloading at the same strain rate of monotonic test up to increasing levels of deformation in order to investigate damage evolution and deviations from the primary path.

The methodology adopted for equibiaxial testing is the bulge test. It consists of blocking between two clamping flanges a thin rubber disc, and inflating with liquid from one side of the specimen until it assumes a "balloon like" shape. The strain field is evaluated by an optical device that measures the deformation of a grid of circular markers previously painted on the specimen surface.The optical setup is composed by two high resolution CMOS cameras Pixelink® B741F with a resolution of 1280×1024. Cameras are fixed on a moveable arm in order to maintain a good focal distance during the inflation of the specimen. During the test an hydraulic circuit inflates or deflates the specimen and cameras grab images of the top of the bulge. The software elaborates in real time the images giving 3D coordinates of markers. For this purpose a previous 3D calibration of cameras is required. From 3D coordinates of markers it is possible, applying a grid method algorithm, to calculate the strain field on the specimen and to estimate the radius on the top of the balloon. Knowing the pressure value at each step of acquisition from a transducer it is possible to calculate the stress [4, 15]. At the same way of uniaxial stretching, two tests are performed both in quasi-static conditions (strain rate in the order of 10^{-3} s^{-1}), one with monotonic loading up to a circumferencial stretch of about 1.8, the other with cyclic loading and unloading up to increasing levels of deformation.

3 HYPERELASTICITY AND PSEUDO-ELASTICITY: BASIC EQUATIONS

Consider a rubberlike continuous body and let $\mathbf{X}$ be the position vectors of its points in the unstressed configuration and $\mathbf{x}$ the correspondent position vectors in the deformed configuration. $\mathbf{X}$ and $\mathbf{x}$ have coordinates X_i and x_j with $i, j \in \{1,2,3\}$. The deformation gradient $\mathbf{F}$ has components $F_{ij} = \partial x_i / \partial X_j$. In the theory of hyperelasticity a strain energy function is defined as $W = W(\mathbf{F})$ and, for isotropic materials, it depends only on the principal stretches $\lambda_1, \lambda_2, \lambda_3$, so that $W = W(\lambda_1, \lambda_2, \lambda_3)$. Furthermore for incompressible materials like rubber it is

$$\lambda_1 \lambda_2 \lambda_3 = 1 \tag{1}$$

and W can be expressed as a function on only λ_1, λ_2. The principal Cauchy stresses are

$$\sigma_i = \lambda_i \frac{\partial W(\lambda_1, \lambda_2)}{\partial \lambda_i} - p \tag{2}$$

where p represents an arbitrary hydrostatic pressure. Avoiding p from equation (2) it is:

$$\sigma_1 - \sigma_3 = \lambda_1 \frac{\partial W(\lambda_1, \lambda_2)}{\partial \lambda_1} \qquad \sigma_2 - \sigma_3 = \lambda_2 \frac{\partial W(\lambda_1, \lambda_2)}{\partial \lambda_2} \tag{3}$$

A very common form of strain energy is the one proposed by Ogden [16]:

$$W(\lambda_1,\lambda_2)=\sum_{p=1}^{N}\mu_p\left(\lambda_1^{\alpha_p}+\lambda_2^{\alpha_p}+\lambda_1^{-\alpha_p}\lambda_2^{-\alpha_p}-3\right)/\alpha_p \tag{4}$$

where N is usually assumed to be 3, α_p and μ_p are real parameters, positive or negative.

In the pseudo-elasticity theory an additional scalar variable is introduced in the strain energy function:

$$W=W(\mathbf{F},\eta)=W(\lambda_1,\lambda_2,\eta) \tag{5}$$

Because of the influence of this new variable we refer now to W as a pseudo-energy function. For isotropic and incompressible material in equilibrium it is:

$$\frac{\partial W(\mathbf{F},\eta)}{\partial\eta}=\frac{\partial W(\lambda_1,\lambda_2,\eta)}{\partial\eta}=0 \tag{6}$$

and stress is given again by (2). During the deformation process η may be either active or inactive and switches between these two states, remaining continuous all the time. When it is inactive the material behaves as an hyperelastic material with the strain energy function $W=W(\mathbf{F},\eta)=W(\mathbf{F},1)$, with η held constant and equal to 1, without loss of generality. When it is active, η can be determined from (6) and in this case it is possible to write $\eta=\chi(\mathbf{F})$. The material will still behave as an hyperelastic material, but with a different strain energy function $W=W(\mathbf{F},\chi(\mathbf{F}))$. According to Ogden and Roxburgh [7], we define the function $\tilde{W}(\lambda_1,\lambda_2)$ as

$$\tilde{W}(\lambda_1,\lambda_2)\equiv W(\lambda_1,\lambda_2,1) \tag{7}$$

that is the energy function of the perfect hyperelastic material expressible as in equation (4). With this function the material will always follow the primary path, also during unloading.

The proposed form of the model is

$$W(\lambda_1,\lambda_2,\eta)\equiv\eta\tilde{W}(\lambda_1,\lambda_2)+\phi(\eta) \tag{8}$$

where $\phi(\eta)$ is called damage function and it is subjected to $\phi(1)=0$. It is clear that, when η is inactive, that is $\eta=1$, this function reduces to (7) describing the primary path. From (8) and (3), stresses are calculated as

$$\sigma_1-\sigma_3=\eta\lambda_1\frac{\partial\tilde{W}(\lambda_1,\lambda_2)}{\partial\lambda_1}\qquad\sigma_2-\sigma_3=\eta\lambda_2\frac{\partial\tilde{W}(\lambda_1,\lambda_2)}{\partial\lambda_2} \tag{9}$$

Substituting (8) into (6) we obtain

$$-\phi'(\eta) = \tilde{W}(\lambda_1, \lambda_2) \tag{10}$$

which implicitly defines the variable η. If $\lambda_{1m}, \lambda_{2m}$ are the stretch values in the point on the primary load from which unload starts, being $\eta = 1$ in that point, it is

$$-\phi'(1) = \tilde{W}(\lambda_{1m}, \lambda_{2m}) = W_m \tag{11}$$

Then it is possible to see that η depends on the specific forms of $\phi(\eta)$ and $\tilde{W}(\lambda_1, \lambda_2)$ and also on the values of $\lambda_{1m}, \lambda_{2m}$. According to the form of $\phi(\eta)$ proposed by Ogden and Roxburgh it is

$$-\phi'(\eta) = \mu \cdot m \cdot \mathrm{erf}^{-1}(r(\eta - 1)) + W_m \tag{12}$$

where m and r are positive dimensionless material constants, μ is the ground state shear modulus ($\mu = 1/2 \sum \mu_p \alpha_p$ for Ogden model) and erf^{-1} is the inverse of the error function. On substitution of (12) into (10) it arises that

$$\eta = 1 - \frac{1}{r}\mathrm{erf}\left[\frac{W_m}{\mu \cdot m}\left(1 - \frac{\tilde{W}(\lambda_1, \lambda_2)}{W_m}\right)\right] \tag{13}$$

and the damage parameter is so defined in an explicit way.

Starting from the previous theory of pseudo-elasticity another variable is introduced to incorporate also the residual strain effect. Thus, the energy function results

$$W = W(\lambda_1, \lambda_2, \eta_1, \eta_2) \tag{14}$$

where η_1 corresponds to the damage variable and η_2 is the residual strain variable. We define the energy function referred to the primary load path, where damage and residual strain variables are inactive, thus equal to 1:

$$\tilde{W}(\lambda_1, \lambda_2) \equiv W(\lambda_1, \lambda_2, 1, 1) \tag{15}$$

When active, variables η_1 and η_2 are implicitly defined by

$$\frac{\partial W(\lambda_1, \lambda_2, \eta_1, \eta_2)}{\partial \eta_1} = 0 \qquad \frac{\partial W(\lambda_1, \lambda_2, \eta_1, \eta_2)}{\partial \eta_2} = 0 \tag{16}$$

while stress is calculated from equations (2, 3) as before. In the work of Dorfmann and Ogden [8] the following pseudo-energy function is proposed:

$$W(\lambda_1, \lambda_2, \eta_1, \eta_2) = \eta_1 \tilde{W}(\lambda_1, \lambda_2) + (1 - \eta_2) N(\lambda_1, \lambda_2) + \phi_1(\eta_1) + \phi_2(\eta_2) \tag{17}$$

where N is the function introduced to characterize the residual strains and ϕ_1 , ϕ_2 are the dissipation functions that are subjected to $\phi_1(1)=0$, $\phi_2(1)=0$. Note that for $\eta_2=1$ equation (17) becomes analogue to (8). From the same authors explicit expressions of η_1 and η_2 , starting with the imposition of specific expressions for ϕ_1, ϕ_2 and substituting them into (16), are given in the form

$$\eta_1 = 1-\frac{1}{r}\tanh\left[\frac{W_m}{m}\frac{1}{\mu}\left(1-\frac{\widetilde{W}}{W_m}\right)\right] \qquad \eta_2 = \tanh\left[\left(\frac{\widetilde{W}}{W_m}\right)^{\alpha}\right]/\tanh(1) \tag{18}$$

where r, m are dimensionless material parameters, μ is the ground state shear modulus, W_m is the potential on the point of the primary path from which unload starts, α is a value that depends on W_m .

According with Dorfmann and Ogden [8] a linear dependence on W_m of the parameter α gives a good approximation. Also a second order law was analysed, but improvements resulted negligible and did not justify the introduction of an additional parameter. Therefore, the law adopted by the authors [17] in the numerical model is

$$\alpha = J + K\left(\frac{W_m}{\mu}\right) \tag{19}$$

where J and K are dimensionless material parameters. For the residual strain function N it has been chosen a model expressed as

$$N(\lambda_1,\lambda_2)=\frac{1}{2}\left[v_1\left(\lambda_1^2-1\right)+v_2\left(\lambda_2^2-1\right)+v_3\left(\lambda_1^{-2}\lambda_2^{-2}-1\right)\right] \tag{20}$$

This is the modified neo-Hookean model as it was proposed by Dorfmann and Ogden [8] that assures negative stress at zero deformation and contemporary takes into account anisotropy by relating the coefficients v_i to the maximum principal stretch applied along the direction i. For these coefficients authors [17] propose the following expression

$$v_i = \mu\left[U - V\tanh\left(\frac{\lambda_{i,m}-1}{Z}\right)\right] \qquad i=1,2,3 \tag{21}$$

where $\lambda_{i,m}$ is the maximum stretch applied along direction i, U, V and Z are three dimensionless material dependent parameters.

Final expressions for stresses will be:

$$\sigma_1-\sigma_3=\eta_1\lambda_1\frac{\partial\widetilde{W}}{\partial\lambda_1}+(1-\eta_2)\lambda_1\frac{\partial N}{\partial\lambda_1} \qquad \sigma_2-\sigma_3=\eta_1\lambda_2\frac{\partial\widetilde{W}}{\partial\lambda_2}+(1-\eta_2)\lambda_2\frac{\partial N}{\partial\lambda_2} \tag{22}$$

For those applications where flat specimens are used, the tensional state can be approximated to biaxial and, defining 3 the direction along the thickness, it is $\sigma_3 \approx 0$. Thus equations (3), (9) and (22) give directly values of σ_1 and σ_2.

Further details and plots regarding the damage variables of the pseudo-elastic model and of its extension for the permanent set are given in [17].

4 NUMERICAL RESULTS

Numerical results and their comparison with test data are presented in this section. All tests have been performed at low strain rate ($\approx 10^{-3}$ s^{-1}) in order to reduce as much as possible any viscoelastic effect. At first, from monotonic loading tests in uniaxial and equibiaxial tension, the Ogden hyperelastic model with N=3 is calibrated in order to fit the points of the primary loading paths. Best-fit parameters are summarized in table 1.

Table 1: Ogden model, N=3. Values of μ_i are in [MPa], α_i are dimensionless.

μ_1	α_1	μ_2	α_2	μ_3	α_3
1.9167	1.6907	-6.7077	-0.9530	9.2209	-0.8103

This set of parameters is obtained by a recursive procedure that minimizes the *RMS* between numerical and experimental data. The *RMS* is evaluated considering both uniaxial and equibiaxial tests data. The same approach will be used to fit cyclic loading tests with pseudo-elastic models, in order to obtain a material model as general as possible, stable and accurate for any heterogeneous tensional state.

Cyclic test data consist on a succession of three full cycles of load-unload up to increasing levels of stretch, and a final load. Figures 2a and 2b show the best fit of cyclic data for uniaxial and equibiaxial tests respectively without considering the residual strain effect (Ogden-Roxburgh model). Curves are obtained with parameter values r = 2.006, m = 0.670 and give a *RMS* = 0.1317 MPa. It is possible to note how this model is not able to fit the quite evident residual strains of the tested rubber. Residual strains can be fitted using the pseudo-elastic model with permanent set and results are given in figures 3a and 3b. In this case more parameters have to be included into the *RMS* minimization procedure. In particular, beside hyperelastic model constants and r and m, there are other five dimensionless parameters to be determined (J, K, U, V and Z). The best fit values of all these material parameters are summarized in Table 2.

Table 2: Material parameters for the pseudo-elastic model with permanent set.
All parameters are dimensionless.

r	m	J	K	U	V	Z
2.559	0.308	0.050	0.054	0.512	1.270	1.693

Fittings of figure 3 show a good correspondence with experimental data and a good capability to fit residual strains. Anyway a small deviation between numerical and experimental data is appreciable in the primary load path at small stretches. This is due to the effort to obtain a general material model, that requires to involve simultaneously in the inverse characterization procedure data coming from different load distributions.

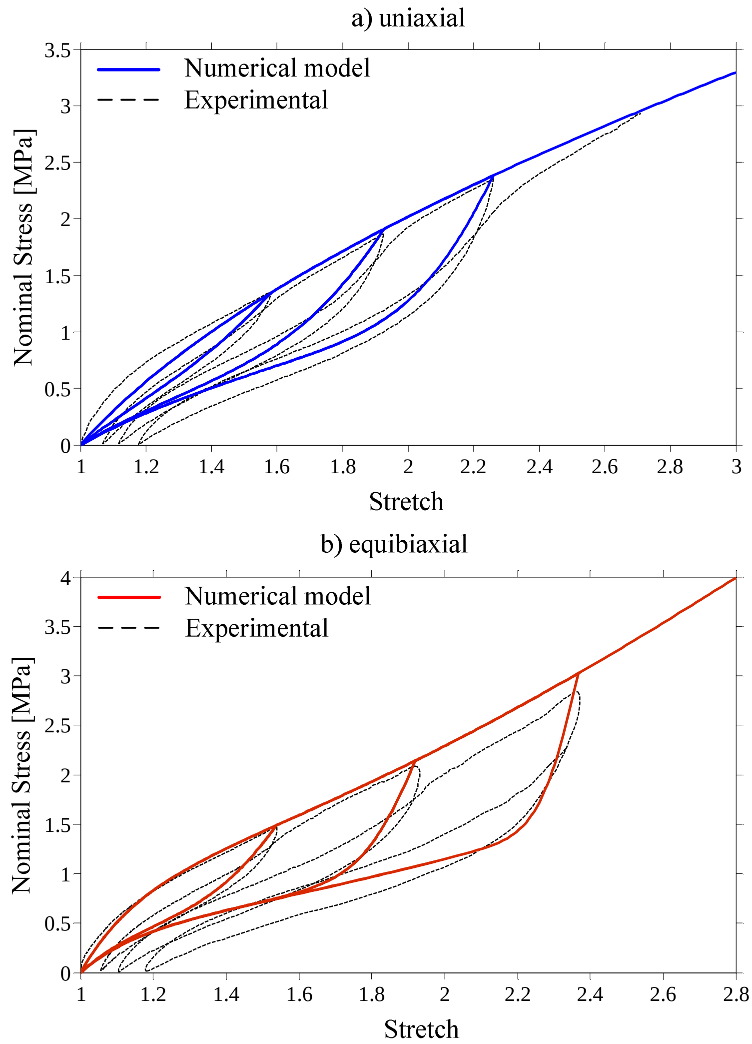

Figure 2: Best-fit curves of Ogden-Roxburgh model, a) uniaxial b) equibiaxial.
Parameters values: μ = 1.081 MPa, r = 2.006 , m = 0.670. RMS = 0.1317 MPa.

A higher accuracy is achievable if one uses only data from uniaxial tests or equibiaxial tests alternatively, as shown in [17]. However this kind of solution may be unstable for other deformational states and the obtained model will be able to work well only in situations that are similar to the one encountered in the calibration tests. From a transferability and generality point of view, an inverse characterization method based on multi-axial deformation data is preferable, and the inaccuracies described above are accepted. Other inaccuracies are due to the hysteresis effect of rubber that makes loading and unloading paths to be different. Models presented in this paper are not able to reproduce this phenomenon, however they give curves that collocate between load and unload. Consequently the approximation results good.

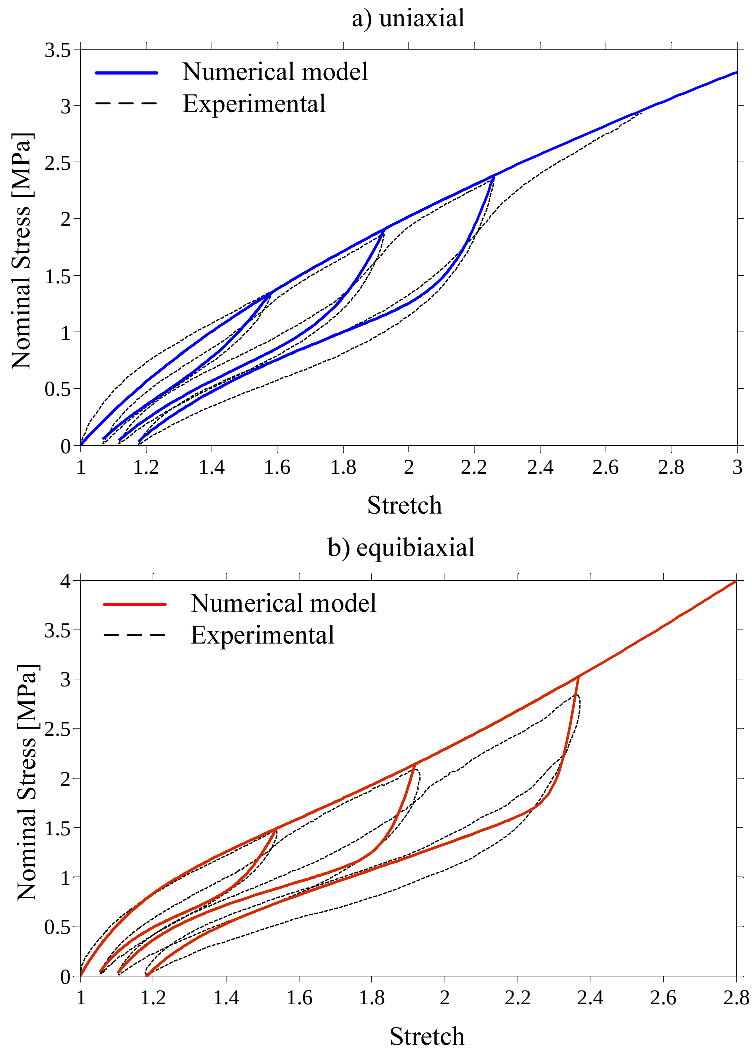

Figure 3: Best-fit curves of pseudo-elastic model with permanent set, a) uniaxial b) equibiaxial. Parameters values are summarized in Table 2. *RMS* = 0.0968 MPa.

5 CONCLUSIONS

Starting from experimental tests of uniaxial and equibiaxial tension on flat rubber specimens, performed by means of test rigs based on optical techniques for strain measurement, a procedure of hyperlelastic and pseudo-elastic models calibration has been developed in order to describe inelastic effects of rubbers, like Mullins effect and residual strain, in a general load distribution.

For the sake of generality and reproducibility, the Ogden-Roxbugrh and the Dorfmann-Ogden methods has been extended with a global multi-axial approach, involving simultaneously uniaxial and equibiaxial test data into the procedure of inverse characterization of the material; moreover, three load-unload cycles have been performed instead of only one. This approach leads to a stable analytical representation of the material behavior for a general state of deformation. Results show a good agreement with experimental data except for small inaccuracies due to the hysteresis of the material, not contemplated in the models.

References

[1] Mooney, M., “A Theory of Large Elastic Deformation,” *Journ. Appl. Phys.*, **11 (9)**, 582-592 (1940).

[2] Treloar, L. R. G., "Strains in an Inflated Rubber Sheet and the Mechanism of Bursting," *Trans.I.R.I.*, **19**, 201-212 (1944).

[3] Rivlin, R.S., "Large Elastic Deformations of Isotropic Materials IV. Further Developments of the General Theory," *Phil. Trans. Roy. Soc. Vol. A*, **241 (835)**, 379-397 (1948).

[4] Sasso, M., Palmieri, G., Chiappini, G., Amodio, D., "Characterization of hyperelastic rubber-like materials by biaxial and uniaxial stretching tests based on optical methods," *Polymer Testing*, **27**, 995-1004 (2008).

[5] Mullins, L., "Effect of stretching on the properties of rubber," *Journal of Rubber Research*, **16**, 275-289 (1947).

[6] Mullins, L., Tobin, N.R., "Theoretical model for elastic behaviour of filler-reinforced vulcanized rubbers," *Rubber Chemistry and Technology Journal*, **30**, 551-571(1957).

[7] Ogden, R.W., Roxburgh, D.G., "A pseudo-elastic model for the Mullins effect in filled rubber," *Proc. R. Soc. Lond. A*, **455**, 2861-2877 (1999).

[8] Dorfmann, A., Ogden, R.W., "A constitutive model for the Mullins effect with permanent set in particle-reinforced rubber," *Int. J. Sol. Struct*, **41**, 1855-1878 (2004).

[9] Beatty, M.F., "The Mullins Effect in a Pure Shear," *Journal of Elasticity*, **59**, 369-392 (2000).

[10] Beatty, M.F., Krishnaswamy, S., "The Mullins effect in equibiaxial deformation," *Z. angew. Math. Phys.*, **51**, 984-1015 (2000).

[11] Johnson, M.A., Beatty, M.F., "The Mullins effect in equibiaxial extension and its influence on the inflation of a ballon," *International Journal of Engineering Science*, **33**, 223-245 (1995).

[12] Qi, H.J., Boyce, M.C., "Constitutive model for stretch-induced softening of the stress–stretch behaviour of elastomeric materials," *Journal of the Mechanics and Physics of Solids*, **52**, 2187-2205 (2004).

[13] De Tommasi, D., Puglisi, G., "Mullins Effect for a Cylinder Subjected to Combined Extension and Torsion," *Journal of Elasticity*, **86**, 85-99 (2007).

[14] Li, J., Mayau, D., Lagarrigue, V., "A constitutive model dealing with damage due to cavity growth and the Mullins effect in rubberlike materials under triaxial loading," *J. Mech. Phys. Solids*, doi:10.1016/j.jmps.2007.06.009, (2007).

[15] Sasso, M., Amodio, D., "Development of a Biaxial Stretching Machine for Rubbers by Optical Methods," *Proc. of SEM Annual Conference*, St Louis (MO), (2006).

[16] Ogden, R.W., "Non-linear elastic deformation," Ellis-Horwood, Chichester, (1984).

[17] Palmieri G., Sasso M., Chiappini G., Amodio D., "Mullins effect characterization of elastomers by multi-axial cyclic tests and optical experimental methods," *Int. J. Mech. Mater.*, doi:10.1016/j.mechmat.2009.05.002, (2009).